Development of a Two-Dimensional Zonally Averaged Statistical–Dynamical Model. Part III: The Parameterization of the Eddy Fluxes of Heat and Moisture

PETER H. STONE

Center for Meteorology and Physical Oceanography, Massachusetts Institute of Technology, Cambridge, Massachusetts and NASA/ Goddard Space Flight Center, Institute for Space Studies, New York, New York

MAO-SUNG YAO

Centel Federal Services Corporation, NASA/Goddard Space Flight Center, Institute for Space Studies, New York, New York

(Manuscript received 25 May 1989, in final form 16 November 1989)

ABSTRACT

A number of perpetual January simulations are carried out with a two-dimensional (2-D) zonally averaged model employing various parameterizations of the eddy fluxes of heat (potential temperature) and moisture. The parameterizations are evaluated by comparing these results with the eddy fluxes calculated in a parallel simulation using a three-dimensional (3-D) general circulation model with zonally symmetric forcing. The 3-D model's performance in turn is evaluated by comparing its results using realistic (nonsymmetric) boundary conditions with observations.

Branscome's parameterization of the meridional eddy flux of heat and Leovy's parameterization of the meridional eddy flux of moisture simulate the seasonal and latitudinal variations of these fluxes reasonably well, while somewhat underestimating their magnitudes. In particular, Branscome's parameterization underestimates the vertically integrated flux of heat by about 30%, mainly because it misses out the secondary peak in this flux near the tropopause; and Leovy's parameterization of the meridional eddy flux of moisture underestimates the magnitude of this flux by about 20%. The analogous parameterizations of the vertical eddy fluxes of heat and moisture are found to perform much more poorly, i.e., they give fluxes only one quarter to one half as strong as those calculated in the 3-D model. New parameterizations of the vertical eddy fluxes are developed that take into account the enhancement of the eddy mixing slope in a growing baroclinic wave due to condensation, and also the effect of eddy fluctuations in relative humidity. The new parameterizations, when tested in the 2-D model, simulate the seasonal, latitudinal, and vertical variations of the vertical eddy fluxes quite well, when compared with the 3-D model, and only underestimate the magnitude of the fluxes by 10% to 20%.

1. Introduction

This is the third paper in a series describing a two-dimensional (2-D), zonally averaged, statistical–dynamical climate model being developed at the Goddard Institute for Space Studies (GISS). This model's structure and parameterizations have much in common with the GISS three-dimensional (3-D) climate model (Hansen et al. 1983). However, the 2-D model is almost two orders of magnitude faster than the 3-D model and therefore can be applied to problems for which the 3-D model is not well suited; e.g., problems requiring many parameter variations, or very long time integrations.

The basic description of the model and the philosophy behind it are given in the first paper in this series (Yao and Stone 1987, hereafter referred to as Part I). A comprehensive review of other 2-D statistical–dynamical models and the history of their development is given by Saltzman (1978). Our model is distinguished from others of the same kind by its inclusion of a comprehensive hydrological cycle and radiation treatment, high vertical resolution (normally nine levels), and by its parameterizations of moist convection and large-scale eddies.

In Part I we developed the moist convection parameterization for our 2-D model. In the second paper in this series (Stone and Yao 1987, hereafter referred to as Part II) we developed the parameterization of the large-scale eddy momentum fluxes. In this paper we concentrate on the development of parameterizations of the eddy fluxes of heat and moisture. The eddy forcing of the zonal-mean zonal-wind and temperature fields is dominated by these fluxes (Edmon et al. 1980; Stone and Salustri 1984). Consequently good parameterizations of these eddy fluxes are crucial for 2-D climate models.

Saltzman (1978) also reviews much of the earlier work on parameterizations of these fluxes. Subsequent to his review, Branscome (1983b) extended earlier pa-

Corresponding author address: Dr. Peter H. Stone, Center for Meteorology and Physical Oceanography, M.I.T., Cambridge, MA 02139.

rameterizations of eddy heat fluxes to include arbitrary values of beta, and his parameterizations will be the starting point for our parameterizations of the eddy heat fluxes. A very recent, independent study by Genthon et al. (1990) has also evaluated the performance of Branscome's parameterizations, using a procedure very similar to the one followed in this paper. Their tests complement ours since there are substantial differences between their model's physics and ours, and since their tests were based on July conditions while ours are based on January conditions. In fact their conclusions concerning Branscome's parameterizations are very similar to ours. Our parameterizations of the eddy moisture fluxes will take the work of Leovy (1973; also see Part II) as their starting point. In the case of the vertical eddy fluxes of both heat and moisture we found it necessary to improve the earlier parameterizations substantially.

The paper is arranged as follows. In section 2 we review our 2-D model. In section 3 we describe the control run used to validate the eddy parameterizations, and how the tests of the eddy parameterizations were carried out. In sections 4, 5, 6 and 7 we describe and test, in order, the individual parameterizations of the meridional eddy heat flux, the vertical eddy heat flux, the meridional eddy moisture flux, and the vertical eddy moisture flux. In section 8 we test all our eddy flux parameterizations simultaneously and discuss our results. The standard symbols used in the mathematical development are defined in the Appendix.

2. Description of the 2-D model

We provide here only a brief outline of our 2-D model. A more complete description can be found in Parts I and II. The model solves the primitive equations (including the moisture conservation equation) in sigma and spherical coordinates as an initial value problem. There are normally nine vertical layers: two in the planetary boundary layer, five in the troposphere, and two in the stratosphere. The model top is at 10 mb, and at higher levels temperatures are determined by radiative equilibrium. There are 24 grid points in latitude, corresponding to a resolution of 7.826°. A time step of 15 minutes was used in Parts I and II, but a time step of 20 minutes is used in this paper. This change has a negligible impact on the simulations, but reduces the computational requirements significantly. The space and time differencing schemes closely parallel those in the GISS 3-D Model II (Hansen et al. 1983), except that an eighth-order Shapiro filter is used to suppress the two-grid-size noise typical of 2-D models. The filter is applied to potential temperature and surface pressure once every hour.

Topography is omitted and surface grid points are divided into land, land-ice, ocean, and sea-ice fractions. In general the sea-ice fraction and the temperatures of the various surface types are calculated interactively. Surface fluxes of momentum, heat, and moisture are calculated separately at each latitude for the different surface types using conventional drag laws. The fluxes for different surface types are then averaged together at each latitude before they interact with the atmosphere.

Incident solar radiation is specified as a function of time of day, season, and latitude. The radiative calculations include all significant atmospheric constituents, and employ realistic short wave and longwave properties. In general, the distributions of water vapor and clouds are calculated, while the remaining radiatively active constituents are specified. Cloud covers are parameterized in terms of relative humidity and cumulus mass flux.

Large scale condensation and precipitation occur in an atmospheric layer whenever the relative humidity exceeds 100%. Moist convection occurs whenever the moist static energy at one level exceeds the saturated moist static energy at the next higher level. The convection is parameterized with a penetrative convection scheme which transports sensible heat, moisture, and horizontal momentum between the unstable layers. Any resulting supersaturation leads to condensation and precipitation. The amount of mixing due to moist convection depends on the fraction of a latitude belt which is unstable, and this is calculated from the zonal variance of the moist static energy. This variance is assumed to arise from eddies generated by baroclinic instability, and it is calculated from parameterizations based on baroclinic stability theory (see Part I).

The large-scale eddy fluxes of momentum, heat, and moisture are in general parameterized, based on the assumption that the eddies arise from baroclinic instability. The parameterization of the eddy momentum fluxes was described in Part II. The parameterizations of the other eddy fluxes will be described in subsequent sections of this paper.

3. Design of the experiments and description of the control run

In order to test parameterizations of the eddy fluxes it is not necessary to use the full generality of our 2-D model as just outlined. Therefore we made the following simplifications for the experiments reported in this paper. The fractional land areas were set equal to zero at all latitudes; the diurnal cycle was omitted; and the sea-ice fractions, sea-surface temperatures, cloud amounts, and all eddy statistics except for the eddy flux which is the subject of the respective experiments, were specified; i.e., held fixed throughout the integrations. The sea-ice fractions and sea-surface temperatures were taken from zonally averaged January mean climatological data. The cloud and eddy statistics were taken from a perpetual January simulation with a semispectral version of the 3-D GISS Model II. This 3-D model differed from the published Model II (Han-

sen et al. 1983) in two respects. First the zonal variations were calculated by means of a spectral expansion which retained the first nine zonal wavenumbers, rather than by finite differencing. Second, all zonal variations were removed from the boundary conditions, i.e., the lower boundary was all ocean having sea-ice fractions and sea-surface temperatures independent of longitude. The 3-D perpetual January simulation used the same values for these boundary conditions as the 2-D experiments. This 3-D control run is described in more detail in Part I.

Since the 3-D simulation contained no nonzonal forcing, the eddy fields it produced are appropriate controls for validating parameterizations of eddy statistics, which are meant to represent eddies arising from baroclinic instability, rather than from topography or land-ocean contrasts. Consequently we will use the eddy heat and moisture fluxes produced by this 3-D simulation as a standard for evaluating our parameterizations of these fluxes. These standard fluxes cannot be compared in detail with observations, because the latter include eddies forced by zonal variations in the boundary conditions, and these eddies in turn are likely to modify eddies arising from baroclinic instability. In particular, there is evidence of strong negative feedbacks between stationary and transient eddy heat fluxes (Manabe and Terpstra 1974; Stone 1984).

Nevertheless, the 3-D model's simulation of the transient eddies can be verified indirectly, by comparing its performance with observations when realistic lower boundary conditions are used in the model simulation. In addition to the 3-D control run described above, we have used the 3-D semispectral model to simulate a calendar January, with realistic lower boundary conditions for continents, topography and sea-surface temperatures—the same boundary conditions as were used in the Model II simulations reported by Hansen et al. (1983). More details of this simulation are given in Parts I and II.

Figure 1 shows the vertically integrated northward transport of heat by all eddies taken from this simulation, and from Oort's (1971) analysis of January observations. Since Oort's analysis did not include results for the Southern Hemisphere, we also include in Fig. 1 the transport by all eddies from Oort and Peixoto's (1983) analysis for the December–January–February season for both hemispheres. We see that the 3-D model simulates the total eddy heat transport accurately in the Southern Hemisphere, but underestimates it by about 30% in the Northern Hemisphere.

The underestimate in the Northern Hemisphere is due to the model's underestimating the transport by stationary eddies rather than by transient eddies. To illustrate this we also include in Fig. 1 the transport by just the transient eddies in the Northern Hemisphere, both from the 3-D simulation with realistic boundary conditions and from observations (Oort 1971). In fact, the 3-D model *overestimates* the transient eddy flux.

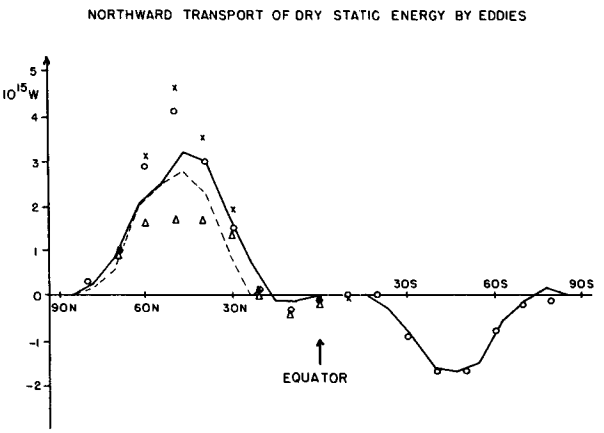

FIG. 1. Vertically integrated January mean northward transport of sensible heat by all eddies (solid line) and by transient eddies (dashed line) from the simulation with the semispectral model using realistic boundary conditions. Also shown are results from observations: the transport by all eddies from Oort and Peixoto (1983) for December–January–February (circles) and from Oort (1971) for January (×'s); and the transports by transient eddies from Oort (1971) for January (triangles).

Since stationary eddies are negligible in the Southern Hemisphere, the good result in the Southern Hemisphere confirms that it is the model's simulation of the stationary eddies that is at fault in the Northern Hemisphere. Experiments with the GISS grid model (Hansen et al., 1983) indicate that the underestimate of the stationary eddy transport in the Northern Hemisphere is due to inadequate horizontal resolution. The GISS grid model with 8° × 10° (latitude by longitude) resolution, which approximates the resolution of the semispectral model with nine zonal wavenumbers, has a similar underestimate of the stationary eddy transport, but this underestimate disappeared when the grid model's resolution was improved to 4° × 5°. We conclude that the 3-D model with nonzonal forcing excluded provides a reasonable control for testing parameterizations of meridional eddy heat fluxes by transient eddies.

Figure 2 shows the vertically integrated northward transport of latent heat by all eddies taken from the 3-D January simulation with realistic boundary conditions. For comparison we include the same transport based on observations, for January in the Northern Hemisphere (Oort 1971), and for the December–January–February season in both hemispheres (Oort and Peixoto 1983). The observational analyses and model results both show that the stationary eddies contribute relatively little to this transport, and thus the comparison of the total transports shown in Fig. 2 in effect tests the 3-D model's ability to simulate the transient eddy flux of latent heat. In fact we see that the model's transport is about 30% to 40% stronger than the observed transport in both hemispheres. This discrepancy will have to be kept in mind when we compare parameterizations of the eddy latent heat transport with the

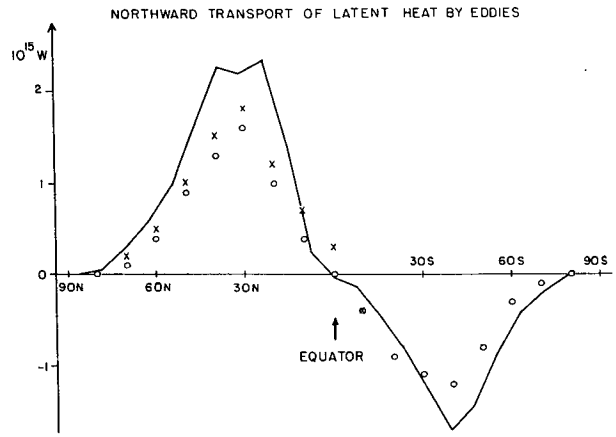

FIG. 2. Vertically integrated January mean northward transport of latent heat by all eddies (solid line) from the simulation with the semispectral model using realistic boundary conditions. Also shown are results from observations for December–January–February (circles) from Oort and Peixoto (1983) and for January (X's) from Oort (1971).

3-D control run. [A similar overestimate is apparent in the results from the GISS grid Model II, Hansen et al. (1983).]

All the 2-D experiments we describe in this paper are perpetual January simulations paralleling the 3-D control run. In all the perpetual January experiments, either 2-D or 3-D, the initial conditions were actual data for 1 December 1976, and the integrations were carried out for eight months, sufficient for an equilibrium climatology to be established. All the fields shown from these experiments are time means for the eighth month of these integrations, and all the differences we discuss are much larger than the monthly variations, unless otherwise stated.

In all the 2-D experiments described in sections 4 to 7, all the eddy fluxes except the flux that is the subject to each respective section, were fixed and taken to be equal to the eddy fluxes generated by the 3-D control run. Thus any differences between the 2-D and 3-D simulations due to errors in eddy fluxes other than the one that is the subject of the respective experiments are excluded. On the other hand, errors in other, interactive parameterizations used in the 2-D experiments such as those for moist convection and large-scale condensation, could in principle contribute to differences between parameterized eddy fluxes in the 2-D experiments and the eddy fluxes calculated in the 3-D control run. However, as we showed in Part I, the parameterizations of these other processes led to 2-D simulations of the general circulation and climatology that were in good agreement with the 3-D control run. Thus differences between the 2-D experiments and the 3-D control run will be due primarily to errors in the eddy flux parameterizations. Finally, we note that the experiments, being global and based on January boundary conditions, include both winter and summer conditions, in the Northern and Southern hemispheres, respectively. Thus all the experiments automatically test the respective parameterization's ability to simulate seasonal differences, as well as latitudinal and vertical variations.

4. The meridional eddy heat flux

Branscome (1983b) derived a parameterization of the meridional eddy heat flux in which the vertical structure of the flux is based on an approximate solution for the most unstable mode in the Charney (1947) model of baroclinic instability, and the magnitude of the flux is based on an equipartition assumption for the mean and eddy potential energies, and the eddy kinetic energy. His parameterization for the meridional eddy flux of potential temperature is (standard mathematical symbols are defined in the Appendix)

$$\overline{v'\theta'} = \frac{Agd^2N_w}{\bar{\theta}_w f^2}\left(\frac{\partial\bar{\theta}}{\partial y}\right)_w^2 e^{-z/D} \tag{1}$$

where A is a constant of order unity; the subscript w refers to a weighted vertical mean, defined by

$$x_w = \frac{1}{D}\int_0^\infty xe^{-z/D}dz \tag{2}$$

$$d = \frac{H_w}{1+\gamma} \tag{3}$$

$$\gamma = \frac{\beta N_w^2 H_w}{f^2\left(\frac{\partial\bar{u}}{\partial z}\right)_w} \tag{4}$$

$$D = \frac{H_w}{\sqrt{4K^2+1}-1} \tag{5}$$

and K is the total wavenumber of the most unstable mode, multiplied by NH/f. Since the eddy flux of potential temperature is proportional to the sum of the eddy fluxes of sensible heat and potential energy, and since the latter flux is much smaller than the former (e.g., see Oort and Peixoto 1983) we will generally refer to the θ fluxes, somewhat loosely, as the heat fluxes. In any case it is the θ fluxes that we require for the form of the first law of thermodynamics used in our model (see Part I).

Branscome (1983b) evaluated A by comparing fluxes calculated from Eq. (1) with eddy fluxes calculated from numerical simulations of the nonlinear evolution of baroclinic instabilities. He found $A \approx 0.6$, and we will adopt this value. For the most unstable wavenumber Branscome (1983b) used the approximation

$$K \approx \frac{1+\gamma}{2}. \tag{6}$$

A more accurate approximation for K has since been derived by Wang et al. (1985), namely

$$K^2 = \frac{(1+\gamma)^2}{\eta^2} - \frac{1}{4} \tag{7}$$

where $\eta \approx 1.35$. At Branscome's suggestion, (personal communication 1988) we have adopted this more accurate approximation. Substituting (7) into (5), we obtain

$$D \approx \frac{H_w}{1.48\gamma + 0.48}. \tag{8}$$

Finally, Branscome's parameterization, like the Charney model, neglects dissipative effects in the planetary boundary layer. When these effects are included in the Charney model, they suppress the meridional eddy heat flux in the boundary layer (Branscome et al. 1989), but have relatively little effect on the structure of the flux above the boundary layer (Lin and Pierrehumbert 1988; Branscome et al. 1989). Thus to model the effect of dissipation we assume that the flux given by Eq. (1) is cut-off exponentially in the boundary layer; i.e., we multiply Eq. (1) by $\{1 - \exp[-(z/\Delta z)]\}$. Meridional eddy heat fluxes calculated from observations (Oort and Peixoto 1983) indicate that an appropriate value of Δz to model the depth of the boundary layer in the eddy heat flux is $\Delta z \approx 450$ m. We shall adopt this value for our parameterization. If we make the above changes in Branscome's original parameterization, Eq. (1) is replaced by

$$\overline{v'\theta'} = 0.6\,\frac{gd^2N_w}{\bar{\theta}_w f^2}\left(\frac{\partial\bar{\theta}}{\partial y}\right)_w^2 e^{-(z/H_w)(1.48\gamma+0.48)} \times [1 - e^{-(z/\Delta z)}]. \tag{9}$$

In applying this parameterization (and indeed all our other parameterizations based on baroclinic stability theory) we require that $(\partial\bar{u}/\partial z)_w > 0$; i.e., if $(\partial\bar{u}/\partial z)_w < 0$ we set $\overline{v'\theta'} = 0$.

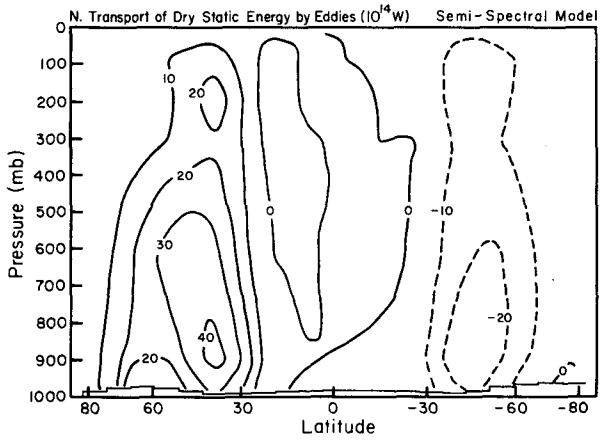

FIG. 3. Pressure latitude cross-section of the total northward transport of dry static energy by eddies from the 3-D control run. Units are 10^{14} W per unit sigma.

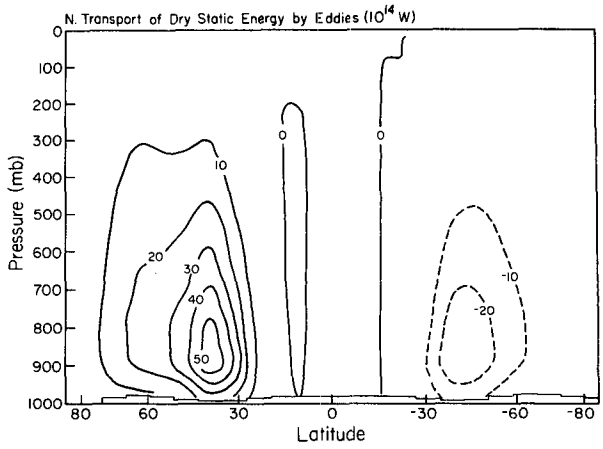

FIG. 4. Same as in Fig. 3, but from the 2-D model using Eq. (9).

Branscome tested his original parameterization by comparing the results it gave with observations. The modifications we introduced above have rather minor effects on the overall parameterization, and so his comparison is also a valid test for our form of his parameterization, Eq. (9). His comparison showed that the parameterization gave reasonable results, if the results were compared with the observed *total* eddy flux (transient plus stationary eddy flux). The problem of interpreting the results of the parameterization when stationary eddies are present can be avoided by applying it in our 2-D model, and comparing it with the eddy flux calculated in our 3-D control run, where stationary eddies were excluded a priori.

Figure 3 shows the eddy heat flux calculated in the 3-D control run, while Fig. 4 shows that the heat flux calculated using Eq. (9) in the 2-D model. The parameterization reproduces the magnitude and the latitudinal and seasonal differences in the eddy heat flux quite well. The main discrepancy is that the parameterization misses the secondary maximum in the flux near the tropopause in both hemispheres. Branscome (1983b) pointed out the same discrepancy. Figure 5 compares the vertically integrated eddy heat flux from the same two integrations. The parameterization significantly underestimates the total heat transport in the summer hemisphere by about 30%, because of the missing secondary flux maximum near the tropopause. Except for the absence of the secondary maximum the parameterization performs quite well, and we will adopt it for our 2-D model.

Changing the approximation for the most unstable mode in the Charney model from Eq. (6) to Eq. (7) had relatively little effect on the meridional eddy heat flux. This change by itself caused the flux to be somewhat more concentrated near the ground, and decreased the vertically integrated flux by about 15%.

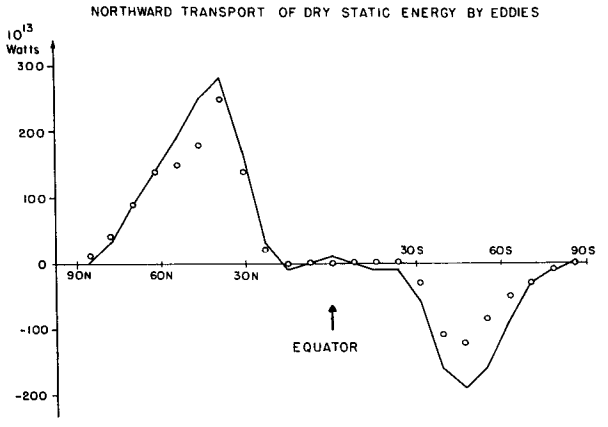

FIG. 5. Vertically integrated northward transport of dry static energy by eddies from the 3-D control run (solid line) and from the 2-D model using Eq. (9) (circles).

However, the new vertical scale given by this change, Eq. (8), differs from the vertical scale in parameterizations of other baroclinic wave properties that we introduced in Parts I and II. Thus we carried out some additional 2-D experiments to see how those parameterizations were changed when the new vertical scale is adopted.

The moist convection parameterization developed in Part I uses a parameterization of latitudinal temperature variance, which was also based on Branscome's work. In that parameterization, given in Eqs. (8) and (10) of Part I, $(z/H_w)(1+\gamma)$ must now be replaced by z/D with D given by Eq. (8) above. The impact of this change, as measured by either the changes in moist convective heating, or by changes in the general circulation, were not significant, with one notable exception. In the Southern Hemisphere subtropics the heating rates were systematically increased by about 10%, and correspondingly the mass circulation in the Southern Hemisphere Hadley Cell increased from 56 to 76 $\times 10^9$ kg s^{-1}. Since the mass circulation in the 3-D control run was 73 $\times 10^9$ kg s^{-1}, this change represented a significant improvement in the moist convection parameterization. Thus we will also adopt the new vertical scale in our moist convection parameterization.

The parameterization of the meridional eddy flux of momentum developed in Part II made use of a baroclinic mixing coefficient that was also based on Branscome's work. The vertical scale of this parameterization can be changed to the new scale by replacing z/d in the exponentials in Eqs. (5) and (6) of Part II by z/D. (We note that the d in the coefficient of Eq. (5) in Part II was inadvertently defined incorrectly. The correct definition is Eq. (3) of this paper, not Eq. (7) of Part II. The correct definition was used in all the calculations of Part II.) The impact of this change is illustrated in Fig. 6. This figure shows the vertically integrated meridional eddy flux of momentum from the 3-D control run, from the 2-D experiment E of Part II, and from experiment E repeated with the new vertical scale replacing the old. (Experiment E contained the final parameterization given in Part II for the meridional eddy momentum flux.) Figure 6 shows that the magnitude of the parameterized eddy momentum flux is significantly increased by changing to the new vertical scale.

In the Northern Hemisphere this increase is an improvement, but in the Southern Hemisphere it is not. In Part II we found that the eddy momentum flux in the subtropics of the Southern (summer) Hemisphere was sensitive to the decay scale we chose for eddy mixing in the tropical easterlies, and that a decay scale of 626 km gave good results. The results illustrated in Fig. 6 indicate that a shorter decay scale would be more appropriate. Thus the last 2-D experiment, using the new vertical scale, was repeated, but with the decay scale for eddy mixing in the tropical easterlies halved to 313 km.

The results of this experiment are also included in Fig. 6. The new decay scale restores the peak values of $\overline{u'v'}$ in both hemispheres to values similar to those found in experiment E in Part II; i.e., in both hemispheres the peak values are now about two thirds of those in the 3-D control run. However, the values are increased somewhat in higher latitudes, and decreased somewhat in lower latitudes. These latter changes improve the agreement with the 3-D control run. The combined changes in the vertical scale and the decay scale also improved significantly the simulation of the Ferrel cells, which had only about one half their proper strengths in the original experiment E (see Part II). In particular the above changes in the parameterization of $\overline{u'v'}$ increased the mass circulation in the Ferrel cells

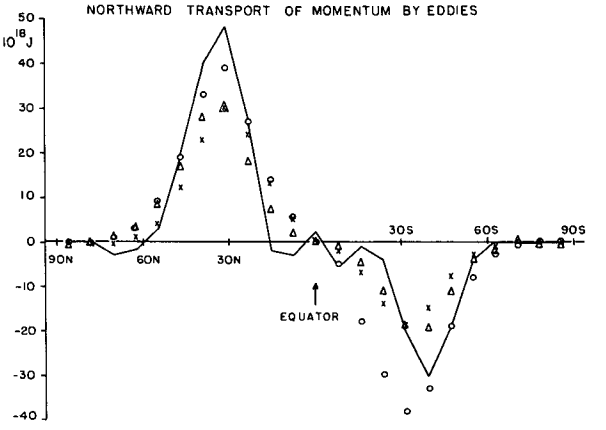

FIG. 6. Vertically integrated northward transport of momentum by eddies versus latitude from the 3-D control run (solid line), the 2-D experiment E of Part II (×'s), the 2-D experiment E repeated with the vertical scale in the parameterization changed to that given by Eq. (8) (circles), and this last 2-D experiment repeated with the decay scale for the eddy mixing in tropical easterlies changed to 313 km (triangles).

by 25% to 30%. Thus we will adopt the new decay scale, 313 km, as well as the new vertical scale, in our parameterization of the eddy momentum flux.

5. The vertical eddy heat flux

Branscome (1983b) also derived a parameterization for the vertical eddy heat flux based on the same assumptions as his parameterization of the meridional eddy heat flux, namely,

$$\overline{w'\theta'} = \frac{-Ag^2d^2}{\bar{\theta}_w^2 N_w f^2}\left(\frac{\partial\bar{\theta}}{\partial y}\right)_w^3\left\{\frac{z}{D} - \frac{z^2}{4D^2}\right\}e^{-z/D}. \quad (10)$$

We will again adopt $A = 0.6$, and the value of D given by Eq. (8) in applying this parameterization. However, we did not believe it was necessary to introduce any boundary layer correction in this parameterization, since the vertical flux is already suppressed in the boundary layer by the rigid boundary condition on w at the ground.

There are no observations of large scale vertical eddy heat fluxes available, so Branscome compared results obtained with Eq. (10) with vertical eddy heat fluxes calculated with the Community Climate Model (CCM) of the National Center for Atmospheric Research (NCAR). He found that his parameterization tended to underestimate the vertical transient eddy heat fluxes in the NCAR CCM, particularly in summer. To test Branscome's parameterization we used Eq. (10) in an experiment with our 2-D model. The vertical eddy heat transport from the 3-D control run is shown in Fig. 7, and the same flux from the 2-D experiment using Eq. (10) in Fig. 8. The peak fluxes based on the parameterization are only about 45% of those in the control run, in both hemispheres. Nevertheless the latitudinal, seasonal, and vertical variations are reasonable. The globally integrated vertical heat transports by the eddies are compared in Fig. 9. The peak in the parameterized

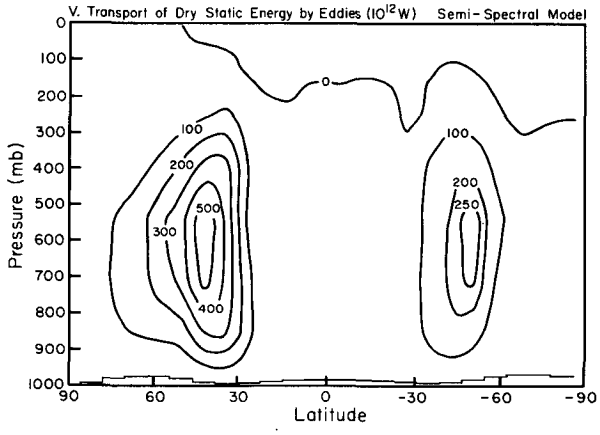

FIG. 7. Pressure–latitude cross section of the vertical transport of dry static energy by eddies from the 3-D control run. Units are 10^{12} W per latitude grid point.

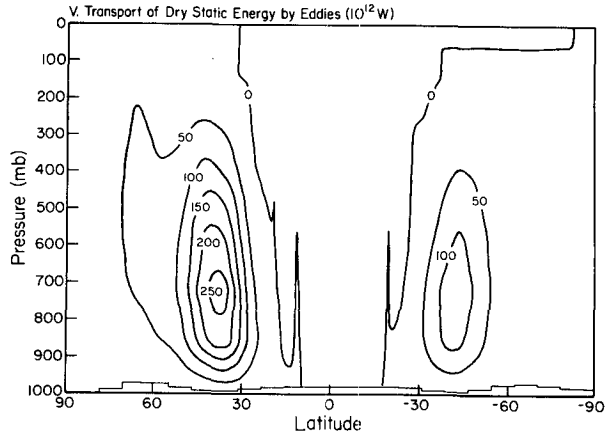

FIG. 8. Same as in Fig. 7, but from the 2-D model experiment using Eq. (10).

global transport is only 42% of that in the control run. Thus our results reinforce Branscome's, that his parameterization of the vertical eddy flux significantly underestimates the flux when compared with more realistic calculations.

We also note that, since there was no equivalent underestimate of the peak in the meridional eddy flux by Branscome's parameterization, the underestimate is primarily due to the *ratio* of the parameterized vertical and meridional eddy fluxes being too small. The parameterizations' ratio is independent of the equipartition assumption, and embodies the normal result found for the most unstable baroclinic wave that the mixing slope near the steering level is about one half the slope of the isentropes (Green 1970; Branscome 1983b). Thus the results from the 3-D control run (and the NCAR CCM) indicate that the effective mixing

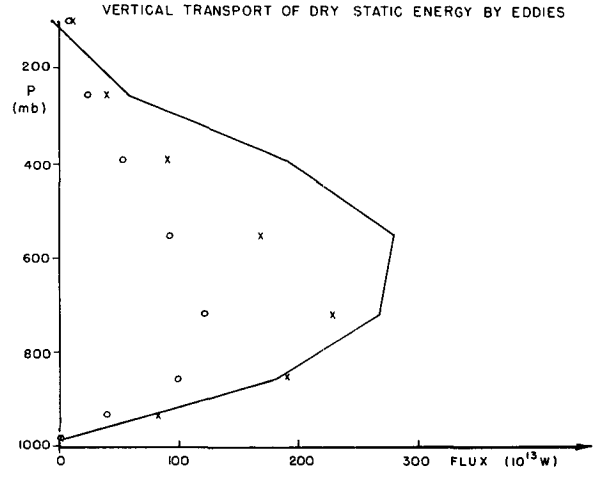

FIG. 9. Globally integrated vertical transport of dry static energy by eddies versus pressure from the 3-D control run (solid curve), from the 2-D model experiment using Eq. (10) (circles), and from the 2-D model experiment using Eq. (22) (×'s).

slope for the eddies is considerably larger than that expected from classical models of baroclinic instability.

Branscome (1983b) suggested that the vertical eddy flux might be enhanced by latent heat release, which is of course neglected in classical models of baroclinic instability. This idea is supported by Held's (1978b) study of the effect of adding a hydrological cycle to a dry two-layer climate model. He calculated the ratio of the mean vertical eddy heat flux, weighted by the static stability, to the mean meridional eddy heat flux, weighted by the meridional gradient of potential temperature. This ratio approximates the mixing slope divided by the isentropic slope. Held found that this ratio (which can only be calculated at 500 mb in his two layer model) was 0.55 in his dry model, close to the value given by classical theories of baroclinic instability, but increased to 0.90 in his moist model.

Additional support for Branscome's suggestion comes from a recent analysis by Emanuel et al. (1987) of how the baroclinic stability problem is modified when condensation occurs in the updraft portion of a growing baroclinic wave. They used a two-layer semi-geostrophic model on an f-plane, and assumed that the growing wave had no cross-stream variations, like the most unstable wave in classical models. This allowed them to calculate the evolution at finite amplitudes. In order to taken into account the effect of condensation in the updraft region they assumed that the updraft remains exactly saturated, and were then able to show rigorously that the effect of the condensation could be modeled by replacing the diabatic thermodynamic equation by an adiabatic thermodynamic equation with a reduced effective static stability. Their solution for the most unstable mode then depended on a single parameter, r, which is, in effect, the ratio of the reduced, effective static stability in the updraft region to the conventional static stability in the unsaturated downdraft region. They found that saturation in the updraft region had very little effect on the temperature and meridional velocity fields but concentrated and intensified the vertical motions, and increased the growth rates. For example, when $r = 0.1$, a typical midlatitude value, the maximum growth rate was increased by about 60%.

Emanuel et al. (1987) did not calculate eddy fluxes or mixing slopes for their solutions, but they provided sufficient information for one case that we were able to do so. This is the case $r = 0.08$, for which they presented graphs of the structure of the most unstable modes. From these graphs we calculated the quantity

$$\rho = \frac{\overline{w'\theta'}}{\overline{v'\theta'}} \frac{N^2}{f\, \partial\bar{u}/\partial z}, \tag{11}$$

i.e., the ratio of the mixing slope to the slope of the isentropes. In our calculation we neglected the distortion of the wave due to finite amplitude effects and we obtained $\rho \approx 1.8$. This may be compared to the value of ρ for the most unstable wave in the dry case, $r = 1$, which is just Phillip's (1954) model. In this latter case $\rho = 2 - \sqrt{2} \approx 0.6$. Thus the effective mixing slope is increased by a factor of about 3 when $r = .08$.

All the above results suggest very strongly that the parameterization of $\overline{w'\theta'}$ needs to be modified to take into account the effect of saturation in the updrafts of growing baroclinic waves. Fantini (1988) devised a method for parameterizing the effect on the growth rate of the most unstable baroclinic wave. He first took the classical result for the growth rate when there is no condensation and the static stability is uniform, and evaluated this result separately for the static stability of the downdraft region and for the reduced effective static stability of the updraft region. He then combined these two growth rates by calculating their average, weighted by the width of the downdraft and updraft regions, respectively. He found that the result reproduced quite well the growth rates found by Emanuel et al. (1987). We will use this same approach to parameterize the effect of saturation on the mixing slope.

To start we will derive the parameterization for a two-layer model on an f-plane. The classical result for the mixing slope at the interface between the two layers for the most unstable wave is

$$\frac{\overline{w'\theta'}}{\overline{v'\theta'}} = (2 - \sqrt{2}) \frac{f}{N^2} \frac{\partial\bar{u}}{\partial z}. \tag{12}$$

If we specify that the Brunt–Väisälä frequency, N, is always defined in terms of the conventional static stability, then Eq. (12) is the conventional result for the mixing slope, evaluated in terms of the static stability of the downdraft region. If we reevaluate this result using the effective static stability of the updraft region, then N^2 in Eq. (12) is simply replaced by rN^2. If we now define λ to be the ratio of the width of the updraft region to that of the downdraft region, then the weighted average of these two values is

$$\frac{\overline{w'\theta'}}{\overline{v'\theta'}} = (2 - \sqrt{2}) \frac{f}{N^2} \frac{\partial\bar{u}}{\partial z} \chi, \tag{13}$$

where

$$\chi = \frac{1 + r^{-1}\lambda}{1 + \lambda}. \tag{14}$$

Thus χ represents the correction to the dry parameterization that results from condensation in the updraft region. We can check this correction by applying it to the case $r = .08$. From Fig. 3a of Emanuel et al. we read off the value of λ corresponding to $r = .08$ and find $\lambda = 0.20$. From these values we then calculate $\chi = 2.9$, in very good agreement with the result calculated above from the exact solution.

Since λ is itself a function of r, χ is a function of r only. The exact definition of r is given by Emanuel et

al., but for use in a parameterization that is only approximate, we will use the simpler form for r that results when we assume the growing wave is small in amplitude. Then the definition of r reduces to

$$r = \frac{\Gamma_m}{\Gamma_d} \frac{\dfrac{\partial \bar{T}}{\partial z} + \Gamma_m}{\dfrac{\partial \bar{T}}{\partial z} + \Gamma_d} \tag{15}$$

where Γ_d and Γ_m indicate the dry and moist adiabatic lapse rates, respectively. We note that $r = 1$ in a dry atmosphere, and $r = 0$ when the lapse rate is moist adiabatic. Emanuel et al. (1987) found the solution for $\lambda(r)$ numerically, and we have derived a simple empirical formula for $\lambda(r)$ which fits their solution, shown graphically in Fig. 3a of their paper, with an accuracy of 4% or better. The formula is

$$\lambda = \frac{0.573\sqrt{r}}{1 - 0.427r^{0.302}}. \tag{16}$$

Emanuel et al.'s (1987) solutions have a singularity at $r = 0$. In this limit the width of the updraft region $\to 0$ and they noted that the semigeostrophic approximation breaks down. There is a corresponding singularity in our parameterization for χ, if Eq. (16) is substituted in Eq. (14). Fantini (1988) investigated what happens when $r \to 0$ by using a numerical primitive equation model in place of the semigeostrophic model. He found that ageostrophic effects removed the singularity; i.e., as $r \to 0$, the updraft region retained a finite width, the most unstable wavelength was about 3000 km, and the mixing slopes were only magnified about 2.5 times, compared to the case $r = 1$ (Fantini 1988, personal communication). We therefore remove the singularity in χ by coupling Eq. (14) with the restriction

$$r \geq r_c \equiv 0.10. \tag{17}$$

This limiting value of r corresponds to $\chi = 2.68$.[1]

The parameterization for the mixing slope at the midlevel of a two-layer model, Eq. (13) and (17), can easily be generalized to a model continuous in the vertical, so long as one retains the restriction $\beta = 0$. First we note that Emanuel et al. (1987) extended their analysis by performing numerical calculations with a multilevel Boussinesq semigeostrophic model, and found that the most unstable mode's steering level remained at the mid level and the largest vertical velocities remained near this level even when $r = 0.1$. This indicates that Eq. (13) is equivalent to a parameterization for the mixing slope at the steering level. Next we note that Branscome's parameterization for the mixing slope yields a vertical structure when $\beta = 0$ consistent with the two-layer model structure, if one allows for the fact that his parameterization is based on a quasi-Boussinesq model with density decreasing exponentially with height, rather than a Boussinesq model. In particular, his parameterization for the mixing slope in the absence of condensation is given by Eq. (10) divided by Eq. (1),

$$\frac{\overline{w'\theta'}}{\overline{v'\theta'}} = \frac{-g}{\bar{\theta}_w N_w^2}\left(\frac{\partial \bar{\theta}}{\partial y}\right)_w \frac{z}{D}\left(1 - \frac{z}{4D}\right)$$

$$= \frac{f}{N_w^2}\left(\frac{\partial \bar{u}}{\partial z}\right)_w \frac{z}{D}\left(1 - \frac{z}{4D}\right). \tag{18}$$

For $\beta = 0$, $D = 2.08H$ and the steering level in Charney's model is at $z/D \approx 0.60$ (Branscome 1983a). Thus at the steering level, for $\beta = 0$, Eq. (18) reduces to

$$\frac{\overline{w'\theta'}}{\overline{v'\theta'}} = 0.51 \frac{f}{N_w^2}\left(\frac{\partial \bar{u}}{\partial z}\right)_w,$$

which is in good agreement with Eq. (13) when $r = 1$. We now obtain a parameterization valid for all r and for a continuous vertical structure by simply combining Branscome's vertical structure with the parameterization valid at the steering level, Eq. (13). This yields

$$\frac{\overline{w'\theta'}}{\overline{v'\theta'}} = \frac{f}{N_w^2}\left(\frac{\partial \bar{u}}{\partial z}\right)_w \frac{z}{D}\left(1 - \frac{z}{4D}\right)\chi(r), \tag{19}$$

where, for the moment, it is understood that this only applies when $\beta = 0$. Since r is a constant in the Emanuel et al. model, we redefine r for a vertically continuous atmosphere by using vertically weighted mean values in Eq. (15). Thus we replace Eq. (15) by

$$r = \frac{(\Gamma_m)_w}{(\Gamma_d)_w} \frac{\left(\dfrac{\partial \bar{T}}{\partial z}\right)_w + (\Gamma_m)_w}{\left(\dfrac{\partial \bar{T}}{\partial z}\right)_w + (\Gamma_d)_w}. \tag{20}$$

Finally, we need to generalize the modified parameterization of the mixing slope so that it is valid for all β. Unfortunately no analysis like Emanuel et al.'s has been carried out for $\beta \neq 0$, so we must be more speculative in our generalization to arbitrary values of β.

[1] After submitting this paper for publication we received from Fantini a preprint in which he reformulated Emanual et al.'s model for the linearized stability problem by using the primitive equations (Fantini 1990). His results show that, if the Rossby number is small, the Emanuel et al. results and our parameterization are still valid, provided that one replaces r by $r + (\partial \bar{u}/\partial z)_w^2/N_w^2$. This replacement obviates the need for the cut-off given in Eq. (17). However it is still appropriate to retain a restriction $r \geq 0$, to parameterize the effect of moist convection in the updraft region of the eddy. This more correct parameterization gave very similar results to those given by the parameterization described in the main text, which was used in all the experiments described in this paper. The footnote in the last section describes the differences caused by changing to the more correct parameterization.

We note that in the classical models of baroclinic instability the main effect of β is to decrease the vertical scale of the most unstable mode (Held 1978a). The vertical scale that enters the parameterization of the mixing slope in the absence of condensation, D, has a β dependence given by Eq. (8). We parameterize the effect of condensation on this scale by again using Fantini's method. We estimate two values of D from Eq. (8), one using the normal N^2 in the definition of γ, and the other using rN^2 in place of N^2, and then we calculate a weighted average of these two values. The resulting parameterization for D is

$$D = \frac{H_w}{1+\lambda}\left[\frac{1}{1.48\gamma + 0.48} + \frac{\lambda}{1.48\gamma r + 0.48}\right]. \quad (21)$$

We note that this equation gives values of D that do not differ very much from the values when condensation is neglected, unless $\gamma \gg 1$. For example, if $\gamma = 0$, or $r = 1$, the moist and dry values are the same; and if $\gamma = 1$, for the extreme case $r = 0.1$, the moist value is only 40% larger than the dry value. Since the vertical eddy flux is exponentially small when $\gamma \gg 1$ we will simply adopt the dry value of D, given by Eq. (8), as being an adequate representation of the vertical scale even when condensation occurs. We note that this is consistent with our 3-D numerical experiments; i.e., the mixing slope peaks at about 500 mb in midlatitudes, both in the 3-D control run and in Branscome's parameterization.

D is the only parameter entering the modified parameterization of the mixing slope, Eq. (19), that we would expect to depend on β. In effect, we expect that Emanuel et al.'s results for a Boussinesq fluid on an f-plane will carry over at least approximately to a quasi-Boussinesq fluid on a β-plane, provided only that the vertical scale of their Boussinesq fluid is taken to be the vertical scale of the most unstable mode with density variations and β-effects taken into account. Thus for our general parameterization of the mixing slope when condensation effects are included, we adopt Eq. (19) with D being given by Eq. (8), χ by Eq. (14), λ by Eq. (16), and r by Eqs. (20) and (17). Our final parameterization for $\overline{w'\theta'}$ is then obtained by simply multiplying the mixing slope times Eq. (1) for $\overline{v'\theta'}$. (We note that if we apply Fantini's method to estimate the effect of condensation on the parameterization for $\overline{v'\theta'}$ we find that the effect is completly negligible, because of the weak dependence of $\overline{v'\theta'}$ on N^2.) Thus we obtain

$$\overline{w'\theta'} = -0.6\,\frac{g^2 d^2}{\theta_w^2 N_w f^2}\left(\frac{\partial\bar{\theta}}{\partial y}\right)_w^3 \chi(r)\left[\frac{z}{D} - \frac{z^2}{4D}\right]e^{-z/D}. \quad (22)$$

We tested this parameterization in our 2-D model, and the result for the vertical transport of heat by the eddies is shown in Fig. 10. The globally integrated vertical heat transport by the eddies from this same experiment is included in Fig. 9. We see that the agreement with the 3-D control run is much better than when we used Banscome's parameterization. The peak values of the transport, and the seasonal and latitudinal variations of the transport are all well represented. The main deficiency is that the parameterization underestimates the transport in the upper troposphere, a defect it shares with the parameterization of $\overline{v'\theta'}$. We will therefore adopt Eq. (22) for the parameterization of $\overline{w'\theta'}$ in our 2-D model.

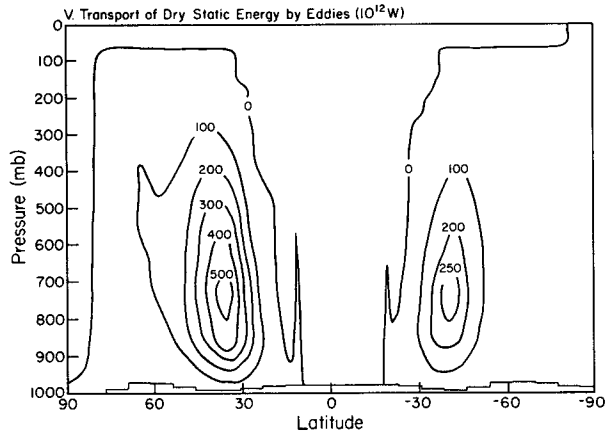

FIG. 10. Same as in Fig. 7, but from the 2-D model experiment using Eq. (22).

6. The meridional eddy moisture flux

Our parameterization of $\overline{u'v'}$ in Part II was based on a generalization of the relationship between the eddy flux of quasi-geostrophic potential vorticity and the Eliassen–Palm flux which allowed one to take into account the effects of condensation. The generalization is based on an approximation of the moisture field suggested by Leovy (1973) and requires a parameterization of $\overline{v'q'}$. The approximation assumes that eddy fluctuations in relative himidity are small compared to fluctuations in specific humidity, and that the Clausius–Clapeyron equation can be linearized. The corresponding parameterization of $\overline{v'q'}$ (see Leovy 1973, and Part II) is

$$\overline{v'q'} = \bar{h}\left(\frac{P}{P_0}\right)^{\kappa}\frac{\partial q_s(\bar{T})}{\partial T}(\overline{v'\theta'}), \quad (23)$$

where h is the relative humidity.

In practice this parameterization is very similar to a diffusive mixing length formulation for $\overline{v'q'}$ (e.g., see Vallis 1982). Since our parameterizations of the eddy fluxes are based on the assumption that they all arise from baroclinic instability, we prefer a parameterization such as the above that ties $\overline{v'q'}$ to $\partial\bar{\theta}/\partial y$ (through $\overline{v'\theta'}$) rather than to $\partial\bar{q}/\partial y$. However, in applying Eq. (23) we do retain one explicit aspect of a diffusive pa-

rameterization; i.e., if Eq. (23) predicts a moisture flux that is *up* the gradient of $\bar{q}$, we set $\overline{v'q'}$ equal to zero rather than using Eq. (23). For realistic climates this rarely happens.

In Part II we tested Eq. (23) by using it to calculate $\overline{v'q'}$ from the mean fields generated in the 3-D control run, and comparing the result with the values of $\overline{v'q'}$ calculated explicitly in the 3-D control run. Unfortunately the calculation of q_s in that test inadvertently omitted the ratio of the molecular weight of water vapor to that of air. As a result, the parameterization appeared to agree with the 3-D calculations better than it should have. (We note however that this error was not made in any of the other calculations in Part II. In particular all the results regarding the parameterization of $\overline{u'v'}$ are correct.) Thus we present here a correct test of Eq. (23).

Figure 11 shows the meridional eddy flux of moisture, in the form of a latent heat transport, from the 3-D control run. Figure 12 shows the same transport calculated using Eq. (23) in a 2-D experiment carried out in the way described in section 3. In this test $\overline{v'\theta'}$ in Eq. (23) was taken from the 3-D control run, so as to eliminate errors in the parameterization of $\overline{v'\theta'}$. We already noted in section 3 one defect in the 3-D model's simulation of $\overline{v'q'}$, namely that it overestimates the vertically integrated transport by 30%–40% (see Fig. 2). Figure 11 illustrates another defect in the 3-D simulation, namely the occurrence of two maxima in $\overline{v'q'}$, one near the surface and another at about 800 mb. This double maximum also appeared in the January simulation with the 3-D model using realistic lower boundary conditions, but does not appear in observations, which show a single peak at about 950 mb (Oort and Peixoto 1983).

The parameterization does not have the second maximum near 800 mb, and in this respect it appears to be superior to the 3-D simulation. In other respects

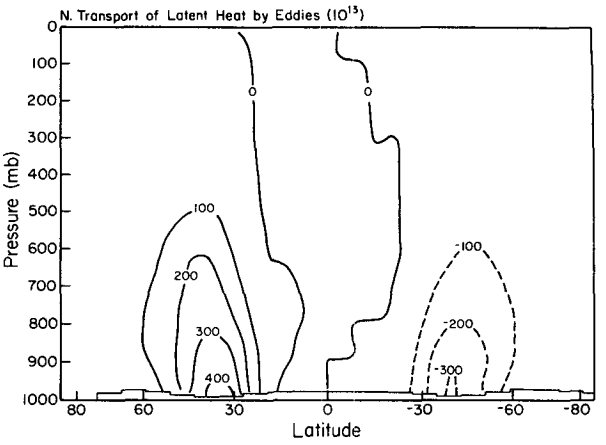

FIG. 12. Same as Fig. 11, but from the 2-D model using Eq. (23).

the parameterization agrees well with the 3-D simulation; e.g., it reproduces accurately the seasonal and latitudinal variations in the transport. Figure 13 shows the vertically integrated meridional transport of latent heat by the eddies from the 3-D control run and from the 2-D experiment. Because the parameterization has no second maximum near 800 mb, it gives a 40% smaller total transport than does the 3-D simulation. However, if we take into account the 3-D model's overestimate of the flux when realistic boundary conditions are used, the parameterized transport appears to be only about 20% too small. Thus the parameterization appears to work well, so far as we can judge it by comparing it with calculations from the 3-D model.

7. The vertical eddy moisture flux

A parameterization of $\overline{w'q'}$ paralleling Leovy's parameterization of $\overline{v'q'}$ can be derived, but tests showed that such a parameterization underestimates the ver-

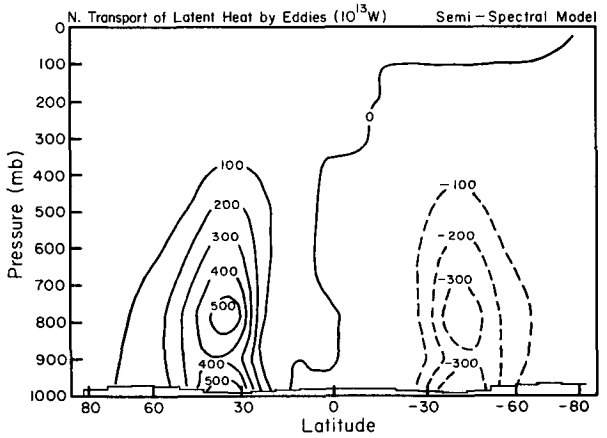

FIG. 11. Pressure–latitude cross section of the meridional transport of latent heat by eddies calculated from the 3-D control run. Units are 10^{13} W per unit sigma.

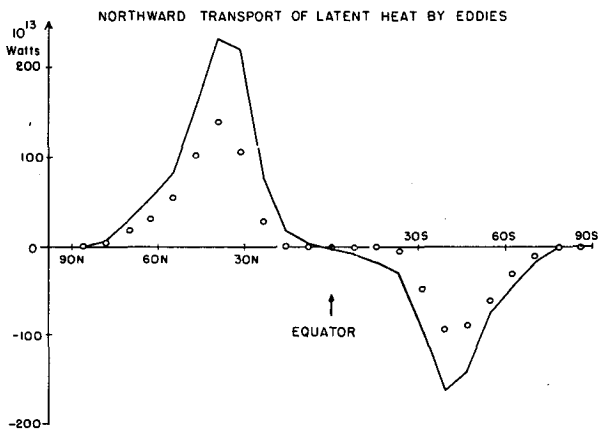

FIG. 13. Vertically integrated northward transport of latent heat by eddies versus latitude from the 3-D control run (solid line), and from the 2-D experiment using Eq. (23) (circles).

tical flux simulated by the 3-D model by a factor of 4. One obvious problem is that the assumption of constant relative humidity is much less realistic for vertical displacements than for horizontal displacements. Another is that condensation should enhance $\overline{w'q'}$ just as it enhances $\overline{w'\theta'}$. Thus to derive a reasonable parameterization for $\overline{w'q'}$ we will first of all derive one that neglects condensation but does not assume constant relative humidity, and then we will modify it to allow for the effects of condensation in the updraft region, using the same method that we used in section 5 for parameterizing the effects of condensation on $\overline{w'\theta'}$.

We derive a parameterization for the case when condensation is unimportant by applying Branscome's (1983b) method for parameterizing $\overline{w'\theta'}$. First we linearize the moisture conservation equation about a mean state consisting of a moisture field, $q(y, z)$, plus a zonal wind, $\bar{u}(y, z)$. We neglect condensation and assume that the perturbation has a normal mode form, $e^{ik(x-ct)}$. The resulting equation for the perturbation moisture field is

$$ik(\bar{u} - c)q' + v'\frac{\partial \bar{q}}{\partial y} + w'\frac{\partial \bar{q}}{\partial z} = 0. \tag{24}$$

Using this equation, we derive the ratio of the vertical eddy moisture flux to the meridional eddy moisture flux,

$$\frac{\overline{w'q'}}{\overline{v'q'}} = \frac{\mathrm{Re}(w'q'^*)}{\mathrm{Re}(v'q'^*)} = \frac{[(\bar{u} - c_r)\,\mathrm{Im}(v'w'^*) + c_i\,\mathrm{Re}(v'w'^*)]\dfrac{\partial \bar{q}}{\partial y} + c_i(w'w'^*)\dfrac{\partial \bar{q}}{\partial z}}{c_i(v'v'^*)\dfrac{\partial \bar{q}}{\partial y} + [(\bar{u} - c_r)\,\mathrm{Im}(v'^*w') + c_i\,\mathrm{Re}(w'v'^*)]\dfrac{\partial \bar{q}}{\partial z}}. \tag{25}$$

To evaluate the coefficients on the right-hand side of Eq. (25) we use Branscome's (1983b) short-wave approximation for the most unstable Charney mode, but with the more accurate value for K given by Eq. (7). With a little algebra we find that this approximation reduces Eq. (25) to

$$\frac{\overline{w'q'}}{\overline{v'q'}} = \frac{f}{N_w^2}\left(\frac{d\bar{u}}{dz}\right)_w \frac{z}{D}\left\{1 + \frac{z}{4D}\frac{f}{N_w^2}\left(\frac{d\bar{u}}{dz}\right)_w \frac{\partial \bar{q}/\partial z}{\partial \bar{q}/\partial y}\right\}. \tag{26}$$

Once again we have identified quantities that are assumed to be constant in the Charney model with vertically weighted averages.

The above parameterization of the mixing slope for the eddy moisture fluxes is closely analogous to Branscome's parameterization of the mixing slope for the eddy heat fluxes, Eq. (18). Indeed, if q is replaced by θ in Eq. (26), it reduces to Eq. (18). Furthermore, q could be replaced by *any* other conservative quantity, and Eq. (26) would then represent a parameterization of the mixing slope for the eddy fluxes of that quantity. Also we note that Eq. (26) did not require us to assume that the relative humidity is constant. Equation (26), coupled with our parameterization of $\overline{v'q'}$, yields a parameterization for $\overline{w'q'}$ when condensation is unimportant.

We tested Eq. (26) by using it to calculate $\overline{w'q'}$ in a 2-D model experiment. Because of the discrepancy between the values of $\overline{v'q'}$ calculated from Leovy's parameterization and the values calculated in the 3-D control run, the values of $\overline{v'q'}$ in this 2-D experiment were set equal to the values calculated with the 3-D model. Thus this experiment tested just the parameterization of the mixing slope for the eddy moisture fluxes. The results were much better than when the $\overline{w'q'}$ parameterization paralleling Leovy's $\overline{v'q'}$ parameterization was used, but the flux was still seriously underestimated, having values 55% to 60% of those calculated in the 3-D model.

To take into account the effect of condensation, we again apply Fantini's method. Now, however, to characterize the situation in the updraft region, we must consider how the moisture conservation equation is modified when the updraft is saturated. This is straightforward, since Emanuel et al.'s (1987) expression for the latent heating due to condensation, their Eq. (9), need only be rewritten as a condensation rate, introduced into the moisture conservation equation, and combined with the vertical advection term to derive an effective vertical moisture gradient. Again we assume that the perturbation amplitude is small. The result for the effective vertical moisture gradient in the saturated updraft region, once again using vertically weighted averages where appropriate, is

$$\left(\frac{\partial \bar{q}}{\partial z}\right)_{\mathrm{eff}} = \frac{C_p}{L}\left[\left(\frac{\partial \bar{T}}{\partial z}\right)_w + (\Gamma_m)_w\right]\left[1 - \frac{(\Gamma_m)_w}{(\Gamma_d)_w}\right]. \tag{27}$$

Thus to characterize conditions in the saturated updraft region we replace N^2 by rN^2, $\partial \bar{q}/\partial z$ by $(\partial \bar{q}/\partial z)_{\mathrm{eff}}$, and $\partial \bar{q}/\partial y$ by $\partial \bar{q}_s/\partial y$.

Making the above replacements in Eq. (26) we calculate a characteristic value of the mixing slope for the updraft region. We then combine that value with the characteristic value for the downdraft region given by Eq. (26) in its original form. When the two values are weighted by the areas of the updraft and downdraft regions, respectively, we obtain

$$\frac{\overline{w'q'}}{\overline{v'q'}} = \frac{1}{1 + \lambda}\frac{f}{N_w^2}\left(\frac{d\bar{u}}{dz}\right)_w \times \left\{\frac{z}{D} + \frac{z^2}{4D^2}\frac{f}{N_w^2}\left(\frac{d\bar{u}}{dz}\right)_w \frac{\partial \bar{q}/\partial z}{\partial \bar{q}/\partial y}\right.$$

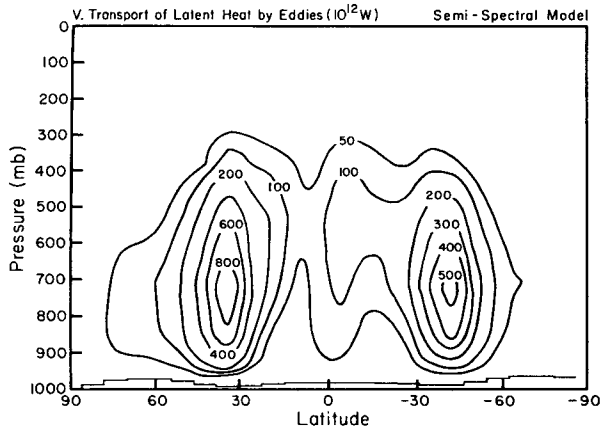

FIG. 14. Pressure–latitude cross section of the vertical transport of latent heat by eddies calculated from the 3-D control run. Units are 10^{12} W per latitude grid point.

$$+\frac{\lambda}{r}\left[\frac{z}{D}+\frac{z^2}{4D^2}\frac{f}{rN_w^2}\left(\frac{d\bar{u}}{dz}\right)_w\frac{(\partial\bar{q}/\partial z)_{\text{eff}}}{\partial\bar{q}_s/\partial y}\right]\Bigg\}. \quad (28)$$

This equation, when coupled with Eq. (23) for $\overline{v'q'}$, gives us our parameterization for the vertical eddy moisture flux. Of course we retain the restriction on r given by Eq. (17).[2]

We performed another experiment with the 2-D model designed to test just the parameterization of the mixing slope for the eddy moisture fluxes, but this time using Eq. (28) in place of Eq. (26). In this test the $\overline{v'q'}$ used to calculate $\overline{w'q'}$ was again set equal to the $\overline{v'q'}$ calculated in the 3-D control run. Figures 14 and 15 show the vertical transport of latent heat by eddies from the 3-D control run and this 2-D experiment, respectively. The parameterization gives spuriously large values in low latitudes because $\partial\bar{q}/\partial y$ and $\partial\bar{q}_s/\partial y \to 0$, whereas $\overline{v'q'}$ remains finite, if small, because of the presence of nonbaroclinic eddies in the 3-D simulations. Thus the low latitude values of $\overline{w'q'}$ calculated from Eq. (28) are omitted from Fig. 15. Comparing Figs. 14 and 15 we see that, in midlatitudes, the parameterization reproduces the magnitude of the flux and its latitudinal, seasonal, and vertical variations rather well. For example the peak values of $\overline{w'q'}$ given by Eq. (28) in midlatitudes is only about 10% to 20% less than the peak values calculated in the 3-D control run.

Finally, we also carried out a 2-D experiment in which the $\overline{v'q'}$ used to calculate $\overline{w'q'}$ from Eq. (28) was parameterized using Eq. (23). The result is shown in Fig. 16. Now there are no spurious values in low latitudes. However the midlatitude fluxes are reduced considerably, because the parameterized $\overline{v'q'}$ is smaller than the $\overline{v'q'}$ calculated in the 3-D model at the levels where $\overline{w'q'}$ peaks. The parameterization again reproduces quite well the latitudinal, seasonal, and vertical variations in $\overline{w'q'}$. Since the discrepancy in the magnitude of the flux appears to be the fault of the 3-D model rather than of the parameterization, as discussed in section 6, we will accept Eq. (28) as a reasonable approximation to use in our 2-D model.

8. Discussion

To test further the parameterizations described in sections 4–7 we carried out another epxeriment. In this experiment the 2-D model was used to simulate perpetual January conditions with *all* the eddy fluxes interacting; i.e., all were calculated simultaneously using the final versions of our parameterizations. We compare the mean eddy fluxes produced in this experiment with those produced in the experiments described in the preceding sections, to see if interactions between the eddy fluxes led to any significant changes in the eddy fluxes.

There was only one significant change in the eddy fluxes in this experiment, namely, the peak value of $\overline{v'\theta'}$ in the winter hemisphere decreased from 56×10^{14} W to 46×10^{14} W. This represents a substantial improvement when compared with the value of 43×10^{14} W in the 3-D control run (cf. Figs. 3 and 4). As a result the vertically integrated meridional sensible heat flux decreased, so that the peak integrated value in the winter hemisphere was 70% of that in the 3-D control run (cf. Fig. 5). Consequently the integrated flux in *both* hemispheres in the interactive experiment was about 30% less than in the 3-D control run.

In both hemispheres this underestimate of the vertical integral of $\overline{v'\theta'}$ is due to the parameterization's lack of a secondary maximum near the tropopause in midlatitude. This lack also causes our parameterization

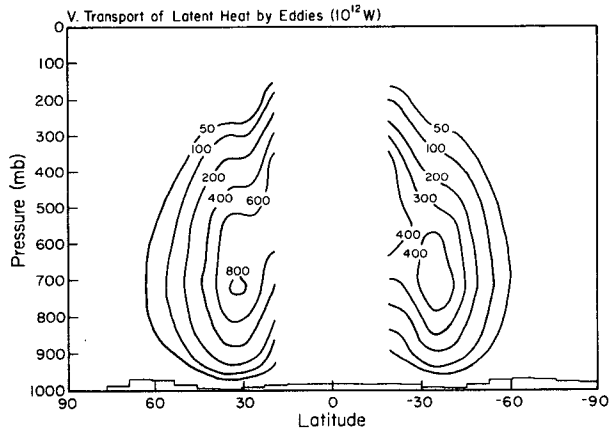

FIG. 15. Same as Fig. 14, but from the 2-D model using Eq. (28) and the $\overline{v'q'}$ calculated in the 3-D control run.

[2] We note again that the more correct way to include the ageostrophic effects that are important when r is small is the way described in the footnote in section 5. When that method is used, the restriction $r \geq 0$ should be accompanied by the parallel restriction $(\partial\bar{q}/\partial z)_{\text{eff}} \geq 0$.

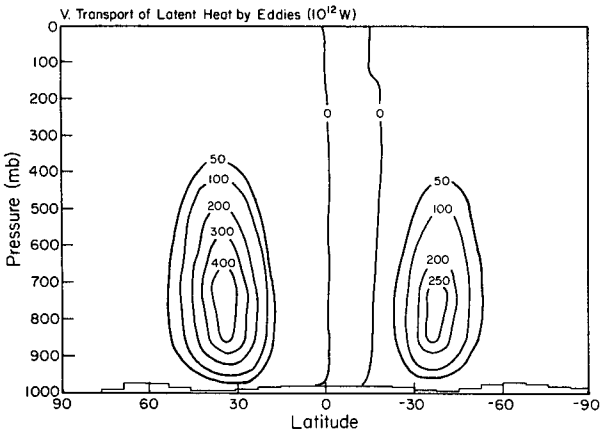

FIG. 16. Same as Fig. 14, but from the 2-D model using Eqs. (28) and (23).

of $\overline{w'\theta'}$ to underestimate its values in the upper troposphere (cf. Fig. 9). Indeed this lack is the one significant defect in our final parameterizations of both the meridional and vertical eddy fluxes of sensible heat. In the lower troposphere, where the primary peaks in $\overline{v'\theta'}$ and $\overline{w'\theta'}$ occur, the errors in the parameterizations are typically only about 10%. The absence of the secondary maximum can be traced to Charney's model of baroclinic instability, which contains no mechanism for concentrating the fluxes in the upper troposphere. It is possible that a more realistic model of baroclinic instability, for example, one that includes a tropopause, could provide the basis for improving these parameterizations.

Evaluating our parameterizations of the eddy moisture fluxes by comparing them with the fluxes calculated in the 3-D control run is more ambiguous, since the 3-D model when integrated with realistic boundary conditions produces a meridional eddy flux with several unrealistic features. In particular, the flux calculated by the 3-D model has two maxima as a function of height, and is too large when integrated vertically. If one makes allowances for these descrepancies, then our final parameterizations for the meridional and vertical eddy fluxes of moisture appear to do reasonably well, with errors on the order of 20%.

Another way of evaluating the parameterizations is to compare the general circulation produced in our 2-D model in the experiment when all the eddy fluxes were parameterized with the general circulation produced in a parallel experiment in which the eddy fluxes are fixed at the values calculated in the 3-D control run. This last experiment with the 2-D model was also carried out. The zonal-mean zonal-winds produced in these two experiments had only minor differences; e.g., the jet stream maxima were reduced by 2 m s^{-1} in both hemispheres, which is not statistically significant. On the other hand there were significant differences in the streamfunction describing the zonal mean meridional and vertical winds in these two experiments. In general the mass circulations were smaller when the eddy fluxes were parameterized, with the mass circulations in both Ferrel cells and in the summer Hadley cell being 30% smaller, and that in the winter Hadley cell being 20% smaller.

An examination of the 2-D experiments in which the individual parameterizations were tested shows that the discrepancies in the meridional and vertical circulations described above were caused primarily by the parameterized magnitude of the meridional eddy flux of momentum being too small (cf. Fig. 6). (Errors in the parameterizations of the meridional eddy fluxes of sensible and latent heat did, however, contribute to the underestimates of the Ferrel cells.) Similar underestimates of the mass circulations due to the underestimate of $\overline{u'v'}$ were illustrated in Part II, in experiment E, where the eddy fluxes of heat and moisture were specified from the 3-D control run. Taken together, the results of all of our experiments show that the main defect in our eddy flux parameterizations is the underestimate of the magnitude of the meridional eddy flux of momentum. In the 2-D model experiment in which all the eddy fluxes were parameterized the peak values of $\overline{u'v'}$ were about 75% of the values in the 3-D control run.[3]

Finally we note that our results concerning the effect of condensation on the vertical eddy fluxes of heat and moisture are important because of what they imply about the effect of eddies on the vertical structure of the atmosphere in midlatitudes. Studies by Stone (1972), Held and Suarez (1978) and Gutowski (1985) have all shown that the vertical eddy fluxes have a significant impact on lapse rates in midlatitudes. However, the first and last of these studies neglected the effects of condensation on the eddy fluxes, and the second did not isolate this effect from the effect of adding a latent heat flux. Our calculations using the Emanuel et al. (1987) model and our 2-D and 3-D climate models indicate that the vertical eddy fluxes of sensible and latent heat are increased by about 100% and 50%, respectively, when the effect of condensation is included. Thus the effect of large scale eddies on midlatitude lapse rates must be enhanced considerably by the effect of condensation.

Indeed this effect offers an explanation for a puzzling result found by Gutowski (1985). He found that the lapse rates calculated by his model agreed best with observed lapse rates when he assumed that the large scale eddies had about 50% more eddy kinetic energy

[3] The experiment with all the eddy fluxes interacting was repeated using the more correct way to limit the singular behavior when $r \to 0$, described in the footnotes in sections 5 and 7. The resulting changes in the eddy fluxes were so small as to be statistically insignificant when compared to the monthly variability. The changes in the general circulation were similarly small. The only change that appeared to be statistically significant, although only marginally so, was that the mass circulation in the summer Hadley cell increased by 10%. This represents an improvement compared to the control run.

than they are observed to have. Since he neglected the impact of condensation on the vertical eddy fluxes, and since he also used Leovy's approximation to parameterize the vertical eddy flux of latent heat, our results indicate that the vertical eddy flux of sensible plus latent heat in his model was only about one-third of what it should have been. Thus the discrepancy in kinetic energy can be explained easily.

Acknowledgments. We are indebted to Lee Branscome for many useful discussions and to Maurizio Fantini for supplying us with some of his unpublished results. This work was supported principally by the NASA Climate Program managed by Robert Schiffer.

APPENDIX

List of Symbols

$( )'$	deviation from the zonal mean
$\overline{( )}$	zonal mean
β	df/dy
c	phase speed in the zonal direction
C_p	specific heat at constant pressure for air
f	Coriolis parameter
g	acceleration of gravity
H	density scale height
κ	R/C_p
k	zonal wavenumber
L	latent heat of evaporation
N	Brunt–Väisälä frequency
p	pressure
P_0	reference pressure
P_s	surface pressure
θ	potential temperature
q	specific humidity
q_s	saturated specific humidity
R	gas constant for air
t	time
u	zonal wind
v	meridional wind
w	vertical wind
x	zonal distance
y	meridional distance
z	height

REFERENCES

Branscome, L. E., 1983a: The Charney baroclinic stability problem: Approximate solutions and model structures. *J. Atmos. Sci.*, **40,** 1393–1409.

——, 1983b: A parameterization of transient eddy heat flux on a beta-plane. *J. Atmos. Sci.*, **40,** 2508–2521.

——, W. J. Gutowski, Jr. and D. A. Stewart, 1989: Effect of surface fluxes on the nonlinear development of baroclinic waves. *J. Atmos. Sci.*, **46,** 460–475.

Charney, J. G., 1947: The dynamics of long waves in a baroclinic westerly current. *J. Meteor.*, **4,** 135–163.

Edmon, Jr., H. J., B. J. Hoskins and M. E. McIntyre, 1980: Eliassen–Palm cross sections for the troposphere. *J. Atmos. Sci.*, **37,** 2600–2616.

Emanuel, K. A., M. Fantini and A. J. Thorpe, 1987: Baroclinic instability in an environment of small stability to slantwise moist convection. Part I: Two-dimensional models. *J. Atmos. Sci.*, **44,** 1559–1573.

Fantini, M., 1988: A study of non-adiabatic baroclinic instability. Ph.D. dissertation, Massachusetts Institute of Technology, 172 pp.

——, 1990: Nongeostrophic corrections to the eigensolutions of a moist baroclinic instability problem. *J. Atmos. Sci.*, **47,** 1277–1287.

Genthon, C., H. LeTreut, J. Jouzel and R. Sadourny, 1990: Parameterization of eddy sensible heat transports in a zonally averaged dynamic model of the atmosphere. *J. Atmos. Sci.*, **47,** in press.

Green, J. S. A., 1970: Transfer properties of the large-scale eddies and the general circulation of the atmosphere. *Quart. J. Roy. Meteor. Soc.*, **96,** 157–185.

Gutowski, W. J., Jr., 1985: A simple model for the interaction between vertical eddy heat fluxes and static stability. *J. Atmos. Sci.*, **42,** 346–358.

Hansen, J., G. Russell, D. Rind, P. Stone, A. Lacis, S. Lebedeff, R. Ruedy and L. Travis, 1983: Efficient three dimensional global models for climate studies: Models I and II. *Mon. Wea. Rev.*, **111,** 609–662.

Held, I. M., 1978a: The vertical scale of an unstable baroclinic wave and its importance for eddy heat flux parameterizations. *J. Atmos. Sci.*, **35,** 572–576.

——, 1978b: The tropospheric lapse rate and climatic sensitivity: Experiments with a two-level atmospheric model. *J. Atmos. Sci.*, **35,** 2083–2098.

——, and M. Suarez, 1978: A two-level primitive equation atmospheric model designed for climatic sensitivity experiments. *J. Atmos. Sci.*, **35,** 206–229.

Leovy, C. B., 1973: Exchange of water vapor between the atmosphere and surface of Mars. *Icarus,* **18,** 120–125.

Lin, S.-J., and R. T. Pierrehumbert, 1988: Does Ekman friction suppress baroclinic instability? *J. Atmos. Sci.*, **45,** 2920–2933.

Manabe, S., and T. B. Terpstra, 1974: The effects of mountains on the general circulation of the atmosphere as identified by numerical experiments. *J. Atmos. Sci.*, **31,** 3–42.

Oort, A. H., 1971: The observed annual cycle in the meridional transport of atmospheric energy. *J. Atmos. Sci.*, **28,** 325–339.

——, and J. P. Peixoto, 1983: Global angular momentum and energy balance requirements from observations. *Adv. Geophys.*, **25,** 355–490.

Phillips, N. A., 1954: Energy transformations and meridional circulations associated with simple baroclinic waves in a two-level quasi-geostrophic model. *Tellus,* **6,** 273–286.

Saltzman, B., 1978: A survey of statistical-dynamical models of the terrestrial climate. *Adv. Geophys.*, **20,** 183–304.

Stone, P. H., 1972: A simplified radiative-dynamical model for the static stability of rotating atmospheres. *J. Atmos. Sci.*, **29,** 405–418.

——, 1984: Feedbacks between dynamical heat fluxes and temperature structure in the atmosphere. *Climate Processes and Climate Sensitivity,* [Americal Geophysical Union, Geophysical Monograph 29], 6–17.

——, and G. Salustri, 1984: Generalization of the quasi-geostrophic Eliassen–Palm flux to include eddy forcing of condensation heating. *J. Atmos. Sci.*, **41,** 3527–3536.

——, and M.-S. Yao, 1987: Development of a two-dimensional zonally averaged statistical-dynamical model. Part II: The role of eddy momentum fluxes in the general circulation and their parameterization. *J. Atmos. Sci.*, **44,** 3769–3786.

Vallis, G. K. 1982: A statistical-dynamical climate model with a simple hydrology cycle. *Tellus,* **34,** 211–227.

Wang, B., A. Barcilon and L. N. Howard, 1985: Linear dynamics of transient planetary waves in the presence of damping. *J. Atmos. Sci.*, **42,** 1893–1910.

Yao, M.-S., and P. H. Stone, 1987: Development of a two-dimensional zonally averaged statistical-dynamical model. Part I: The parameterization of moist convection and its role in the general circulation. *J. Atmos. Sci.*, **44,** 65–82.